



CT-2

HIERARCHICAL SILVER NANOSTRUCTURES PRODUCED BY ELECTROSPINNING AND NOVEL HYDROTHERMAL TREATMENT

Nasser A. M. Barakat and Taha E. Farrag*

ABSTRACT

Silver nanoparticles have been synthesized in a new hierarchical shape using simple electrospinning technique and novel hydrothermal treatment process. A sol-gel consisting of poly(vinyl alcohol) and silver nitrate has been electrospun to produce nanofiber mats which were dried under vacuum at room temperature for 24 h. The dried nanofiber mats have been hydrothermally treated by novel strategy. The treatment process was based on producing of water gas (CO and H₂) to eliminate the polymer and to reduce the silver nitrate into silver metal. The process was carried out by heating the dried nanofiber mats at 300 °C for 30 min in an especially designed reactor in which a stream of water vapor was passing through an activated carbon bed. X-Ray diffraction pattern (XRD) and thermal gravimetric analysis (TGA) have affirmed that the proposed treatment methodology has been completely eliminated the utilized polymer and decomposed silver nitrate into pure silver. Moreover, scanning electron microscope images revealed that the obtained product have novel nanostructure; leaves of date tree shapes. According to the wide application of silver nanostructures, the newly obtained shape may have especial interest to be invoked in several applications.

Keywords

Silver nanoparticles, Hierarchy, Electrospinning, Hydrothermal treatment.

* Chemical Engineering Department, Faculty of Engineering, Minia University, Egypt

1. Introduction

Technology relating to nanoscale materials has become an increasingly important area for technical development, and remains under broad scrutiny for scientific, commercial, and military applications. There are unique physical properties of materials at this scale, and a wide range of potential applications proposed to take advantage of these unique properties. Potential market applications for this technology include smart filters for medical, biological and chemical purposes. Recently, noble metals nanostructures such as silver and gold have gained great interest because of their superior electrical, optical, mechanical, and catalytic properties [1-5]. Surface plasmon resonance (SPR) is one of the most interesting features of these nanoparticles (NPs). SPR is a phenomenon which occurs when light is reflected off thin metal films or NPs. A fraction of the light energy incident at a sharply defined angle can interact with the delocalised electrons in the metal surface (plasmon) thus reducing the reflected light intensity [6].

In particular, silver and gold metals are the most popular materials used in this concern [7], however, silver is most commonly utilized [8], because its *d-s* band gap is in the UV region and does not damp out the plasmon mode as strongly as for gold [9]. Many applications based on SPR feature have been reported, including medical diagnostic and therapeutics [10,11], chemical and biochemical sensors [12,23], substrates for enhanced spectroscopies [14], and light transmission at the sub-wavelength regime [15]. Another advantageous feature of surface plasmon excitations in metallic nanostructures is that the electromagnetic fields propagating in the form of surface plasmon is not diffraction limited, which can be used to create fast optical devices with significantly reduced dimensions.

It has been recently reported that the sensitivity as well as the tunability of the resonance wavelength maximum is closely related to the geometry of the nanoparticles [6,13,16]. Both calculation and experiment proofed that one dimensional (1D) metal NPs reveal a much greater local field enhancement and therefore more significant applications [17,18]. Moreover, the relative ratio of the long axis to short axis for the 1D NPs has especial effect [19]. Therefore, many reports have been introduced for production of silver nanorods [20-23]. Beside the importance of the plasmon resonance feature of the metals NPs colloids, the band gap energy has especial interest in spectroscopy and optical switches applications [24, 25]. Also, the optical properties depends on the particle shape, 1D form reveals high band gap energy [26].

In this study, a new hierarchy have been prepared by novel hydrothermal treatment of nanofiber mats composed of silver nitrate and poly(vinyl alcohol). The nanofiber mats have been treated in an especial reactor.

2. Experimental

2.1 Materials

Silver nitrate (99.8 assay) and poly(vinyl alcohol) (PVA, molecular weight (MW) = 65000 g/mol) were obtained from Showa Co., Japan and Dong Yang Chem. Co., South Korea, respectively. These materials were utilized without any further treatments. Distilled water was used as solvent.

2.2 Procedures

Electrospinning is a process to make nanofibers with fiber diameters in the range of about 10 to several hundreds nanometers from polymer solution through electrostatic force. This technique involves the use of a high voltage to charge the surface of a polymer solution droplet and thus to induce the ejection of a liquid jet through a spinneret. Due to bending instability, the jet is subsequently stretched many times to form continuous, ultrathin fibers. Recently, the electrospinning technique has been exploited to prepare some metals nanofibers [27-29].

In the present study, a sol-gel was prepared by mixing 15 wt% of aqueous silver nitrate solution and 10 wt % of PVA aqueous solution in a ratio of 2:5. The obtained solution was placed in a plastic capillary. A carbon pin connected to a high-voltage generator was inserted in the solution, and the solution was kept in the capillary by adjusting the inclination angle. A ground iron drum covered by polyethylene sheet was serving as a counter-electrode. A voltage of 20 kV was applied to this solution. The distance between the syringe and ground drum was kept at 15 cm as it is the optimum distance to get smooth and well morphology electrospun nanofibers. No feeding pump was invoked. An illustration for the used electrospinning setup is shown in Figure 1. The formed nanofiber mats were initially dried for 24 h under vacuum.

The dried nanofiber mats were hydrothermally treated in especially designed reactor (Figure 2). The reactor was made of stainless steel with height of 15 cm and diameter of 7 cm. The reactor was designed to perform a chemical reaction between the water vapor and hot activated carbon to produce carbon monoxide and hydrogen gases according to the following reaction:



This reaction is well known as water gas reaction. The experiment was conducted as follows: a sealed metallic bottle was filled with water and placed at the bottom of the reactor. An activated carbon (as a source of carbon), and nanofiber mats were placed on two meshes above the metallic bottle as shown in Figure 2. Finally, the reactor was sealed with a stainless steel cover and heated to 300 °C for 30 min. The heating process was achieved in silicon oil bath heated at 300 °C, the sealed reactor was immersed in the hot bath and left for 30 min, then, removed and rapidly cooled by quenching in cold water.

Due to heating of the reactor in the oil bath, the water boiled inside the bottle and the pressure increased. Therefore, water vapor streamed out with small flow rate due to the fixed cover. The hot vapor reacted with the hot carbon layer to produce water gas as indicated in reaction 1. The resulting reducing gases reacted with the nanofiber mats existing on the upper mesh. As time passes, the pressure increased inside the reactor, so some gases escaped from the reactor. No rubber seals were utilized in the cover of either the metallic bottle or the reactor.

3. Characterization

Surface morphology was studied by scanning electron microscope (SEM, JEOL JSM-5900, Japan) and field-emission scanning electron microscope (FESEM, Hitachi S-7400, Hitachi, Japan). In case of the original silver nitrate/PVA nanofiber mats, the mat was coated by gold and low vacuum mode was utilized. Secondary electrons imaging technique was invoked. Information about the phase and crystallinity was obtained by using Rigaku X-ray

diffractometer (XRD, Rigaku, Japan) with Cu K α ($\lambda = 1.540 \text{ \AA}$) radiation over Bragg angle ranging from 10 to 90°. High resolution image and selected area electron diffraction patterns were obtained with transmission electron microscope (TEM, JEOL JEM-2010, Japan) operated at 200 kV. Thermal properties have been studied by thermal gravimetric analyzer (TGA, Pyris1, PerkinElmer Inc., USA).

4. Results and Discussion

The general morphologies of the as-grown products were examined by FESEM and shown in Figure 3. Figures 3A and 3B reveal the SEM images of the dried silver nitrate/PVA nanofiber mats, as shown in these figures; the electrospinning process produced relatively smooth nanofibers with almost 350 nm average diameter. Beads or agglomerated nanofibers can not be observed in the obtained mats. After the proposed hydrothermal treatment methodology, a hierarchical shape has been obtained due to existing of the nanofiber mats under high pressure. Figure 4 demonstrates the SEM images for the obtained product in four magnifications. As shown in this figure, the nano fibrous morphology has been altered to dendrite structure.

The polymer is an essential constituent in the sol-gel to achieve the electrospinning process. PVA does have a wide utilization in producing of metallic nanofibers via electrospinning methodology for its novel chemical and thermal characteristics. The hydroxyl groups deployed on the PVA chains have the capability to generate hydrogen bond with many anions (especially those having oxygen atom) which enhances the solubility of the metal salt in PVA solution. Moreover, PVA has low decomposition temperature, so, elimination of PVA from the obtained electrospun nanofiber mats is an easy task [30]. Likewise, silver nitrate decomposes easily by heat [31]. In the proposed hydrothermal treatment strategy, reduced gases are evolving which enhances elimination of PVA polymer and decomposition of silver nitrate. The typical XRD pattern of the calcined powder at the utilized calcination temperatures is presented at Figure 5. The strong diffraction peaks at 2θ values of 38.25, 44.45, 64.60 and 77.65° corresponding to (111), (200), (220) and (311) crystal planes indicate the formation of crystalline silver metal (JCDPS, card no 04-0783).

Standard silver does have cubic crystal with cell parameter of 0.4086 nm (JCDPS, card no 04-0783). Figure 6 shows the HR TEM image of the obtained product. The top-left inset in this figure shows the FFT image, as shown in this inset; the distance between two successive planes almost matches the standard value; 0.41 nm which indicates good crystallinity of the obtained nanofibers. The top-right inset reveals the SAED pattern. As shown in this inset, SAED pattern reveals good crystallinity at the utilized calcination temperature. There are no dislocations or imperfections observed in the lattice planes which indicate good crystallinity of the synthesized material.

Since XRD and TEM analyses have confirmed that the final obtained product composed of silver nanoparticles, we have invoked TGA analysis in argon atmosphere to decide whether silver metal was produced because of reduction by the synthesized water gas or due to thermal decomposition in oxygen-free atmosphere. Figure 7 shows the thermal gravimetric analysis for silver nitrate/PVA nanofiber mats in argon atmosphere, along with the first derivative was plotted. As shown in the first derivative curve there are some peaks denoting decrease in the weight of the sample. The peak at around 50 °C can be explicated as evaporation of the physical absorbed water in the sample. Another sharp and high depth peak is appeared at ~ 200 °C, with taken in consideration the thermal properties of PVA and its

mass content in the original nanofiber mats; this peak can be characterized by decomposition of PVA. Silver is a noble metal, so, it tends to state at zero oxidation state. However, it is well known that the thermal decomposition depends upon the environment. Therefore, the small peak at around 240 °C might be illustrated as partial decomposition of the silver nitrate according to this reaction



The last broad peak at ~ 340 °C reveals to formation of the silver metal from the inorganic compounds remaining in the sample as follow:



It is noteworthy mentioning that the last reaction is common and cited in the literatures.³¹ According to these results, we can say that the evolved water gas plays an important role in producing of silver metal since our experiment has been conducted at relatively lower temperature (300 °C) than the required one to completely decompose silver nitrate in an inert atmosphere. Our previous work³² about silver nitrate/PVA electrospun nanofiber mats revealed that pure silver metal can be obtained with different treatment process to eliminate the polymer content; for instant calcination in air or in argon resulted in producing of pure silver. This is due to the nobility of the silver metal. It is noteworthy mentioning that according to our pervious study on the same nanofiber mate [32]; calcination in argon atmosphere results in production of silver nanofibers. We think there are two main reasons lead to obtain different morphology in this study; the pressure and degradation rate. In the proposed strategy the sample is treated under high pressure compared with calcination in argon atmosphere process (atmospheric pressure). Also, the degradation rate in case of argon atmosphere calcination process is very low, however, in the proposed hydrothermal strategy it is much higher.

The obtained dendrite structure can be explained according to the characteristics of the electrospinning process and the features of the obtained silver nitrate/PVA nanofiber mats (Figure 3). As it is well known that the diameters of the nanofibers obtained by the electrospinning technique are not constant. In other words, the electrospun nanofibers not have same diameter, they fall in range. Moreover, as shown in Figure 3, the obtained silver nitrate/PVA nanofibers are soldered at the contact points. We can divide the obtained structure into two main parts, a backbone and branches connected with this backbone. The main backbone can be investigated as silver nanofiber obtained from thick silver nitrate/PVA nanofiber, so, the produced silver nanofiber became thick and strong. The original thick polymeric nanofiber does have many other thin fibers merged with it in many places. The obtained silver from these thin nanofibers will be weak and thin, with taken into consideration that silver strongly tends to agglomerate [32], so, these weak nanofibers converted into short and thick parts joint with the mean backbone as leaves.

Finally, the proposed synthesizing strategy does have the following advantages over the reported techniques to produce hierarchical silver nanostructures. Simplicity is the first main advantage accompanying the proposed method. Moreover, low cost is also an important factor for the proposed method. Also, easiness of application is a considerable feature since the required instruments are not sophisticated.

5. Conclusion

Hydrothermal treatment of silver nitrate/PVA electrospun nanofiber mats at high pressure in presence of water gas leads to producing interesting hierarchical shape silver nanoparticles. The reducing power of the evolved water gas causes to complete elimination of the used polymer and decomposition of the silver nitrate into silver metal at relatively low temperature. Presence of the sample in high pressure vessel fast polymer degradation rate enhance attaching the silver nanorods to form date tree leaf-like shape.

References

- [1] M. Bockrath, W. Liang, D. Bozovic, J. H. Hafner, C. M. Lieber, M. Tinkham, and H. Q. Park, *Science*. 291 (2001) 283.
- [2] Y. Cui, Q. Q. Wei, H. Q. Park, and C. M. Lieber, *Science*. 293 (2001) 1289.
- [3] D. Torres, N. Lopez, F. Illas, and R. M. J. Lambert, *Am. Chem. Soc.* 127 (2005) 10774.
- [4] F. J. Williams, D. P. C. Bird, A. Palermo, A. K. Santra, and R. M. Lambert, *J. Am. Chem. Soc.* 126 (2004) 8509.
- [5] A. Tao, F. Kim, C. Hess, J. Goldberger, R. R. He, Y. G. Sun, Y. N. Xia, and P. D. Yang, *Nano Lett.* 3 (2003) 1229.
- [6] C. F. Bohren and D. R. Huffman, *Absorption and Scattering of Light by Small Particles*; Wiley-Interscience: New York, (1983).
- [7] T. Nikolajsen, T. Leosson, K. Salakutdinov, and S. Bozhevolnyi, *Appl. Phys. Lett.* 85 (2004) 5833 (2004).
- [8] C. L. Haynes and R. P. Van Duyne, *J. Phys. Chem. B.* 107 (2003) 7426.
- [9] J. H. Hodak, I. Martini, and G. V. Hartland, *J. Phys. Chem. B.* 102 (1998) 6958.
- [10] I. H. El-Sayed, X. Huang, and M. A. El-Sayed, *Nano Lett.* 5 (2005) 829.
- [11] L. R. Hirsch, R. J. Stafford, J. A. Bankson, S. R. Sershen, B. Rivera, R. E. Price, J. D. Hazle, N. J. Halas, and J. L. West, *Proc. Natl. Acad. Sci. U.S.A.* 100 (2003) 13549.
- [12] A. D. McFarland and R. P. Van Duyne, *Nano Lett.* 3 (2003) 1057.
- [13] L. Cagnet, C. Tardin, D. Boyer, D. Choquet, P. Tamarat, and B. Lounis, *Proc. Natl. Acad. Sci. U.S.A.* 100 (2003) 11350.
- [14] J. Jiang, K. Bosnick, M. Maillard, and L. Brus, *J. Phys. Chem. B.* 107 (2003) 9964.
- [15] J. A. Dionne, L. A. Sweatlock, H. A. Atwater, and A. Polman. *Phys. Rev. B.* 73 (2006) 35407-1.
- [16] G. Raschke, S. Brogl, A. S. Susha, A. L. Rogach, T. A. Klar, J. Feldmann, B. Fieres, N. Petkov, T. Bein, A. Nichtl, and K. Kurzinger, *Nano Lett.* 4 (2004) 1853.
- [17] D.-S. Wang and M. Kerker, *Phys. Rev. B.* 24 (1981) 1777.
- [18] B. Nikoobakht, J. Wang, and M. A. El-Sayed, *Chem. Phys. Lett.* 366 (2002) 17.
- [19] L. Kyeong-Seok and M. A. El-Sayed, *J. Phys. Chem. B.* 110 (2006) 19220.
- [20] A. Kadir, L. Zoya, R. L. Joseph, and D. G. Chris, *J. Phys. Chem. B.* 109 (2005) 3157.
- [21] H. Xin, Z. Xiujian, C. Yunxia, F. Jinyang, and S. Zhenya, *J. Solid State Chem.* 180 (2007) 2262.
- [22] J. L. Gil, I. S. Seung, C. K. Young, and G. O. Seong, *Mater. Chem. Phys.* 84 (2004) 197.
- [23] K. L. Fu, W. H. Pei, C. C. Yu, J. K. Chu, H. K. Fu, and C. C. Tieh, *J. Cryst. Growth.* 273 (2005) 439.
- [24] R. Zai, M. D. Selker, and M. L. Brongersma, *Phys. Rev. B.* 71 (2005) 165431-1.
- [25] M. Hochberg, T. Baehr-Jones, C. Walker, and A. Scherer, *Opt. Express.* 12 (2004) 5481.

- [26] N. A. M. Barakat, M. S. Khil, F. A. Sheikh, and H. Y. Kim, *J. Phys. Chem. C.* 112 (2008) 12225.
- [27] W. Hui, Z. Rui, L. Xinxin, L. Dandan, and P. Wei, *Chem. Mater.* 19 (2007) 3506.
- [28] B. Michael, B. Mathias, G. Martin, M. Werner, H. W. Joachim, S. Andreas, W. Dirk, B. Andre, G. Armin, and G. Andreas, *Adv. Mater.* 18 (2006) 2384.
- [29] M. Graeser, M. Bognitzki, W. Massa, C. Pietzonka, A. Greiner, and J. H. Wendorff, *Adv. Mater.* 19 (2007) 4244-4247.
- [30] D. M. Fernandes, A. A. W. Hechenleitner, E. A. G. Pineda, *Thermochim. Acta.* 441 (2006) 101.
- [31] W. Hui, L. Dandan, Z. Rui, and P. Wei, *Chem. Mater.* 19 (2007) 1895.
- [32] N. A. M. Barakat, K. D. Woo, M. A. Kanjwael, K. E. Choi, M. S. Khil and H. Y. Kim, *J. Phys. Chem.* 24 (2008) 11982.

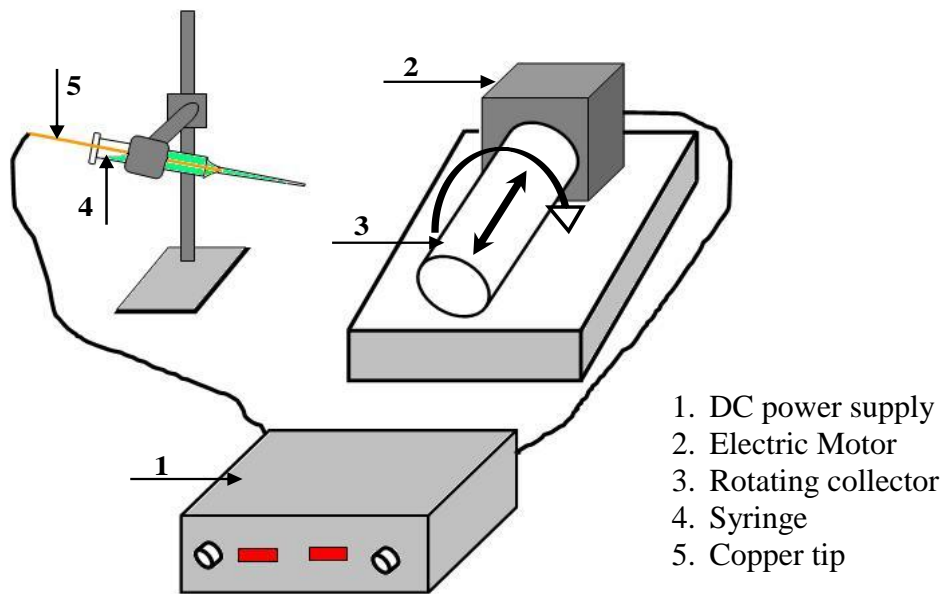


Figure 1: Schematic diagram of a simple electrospinning apparatus

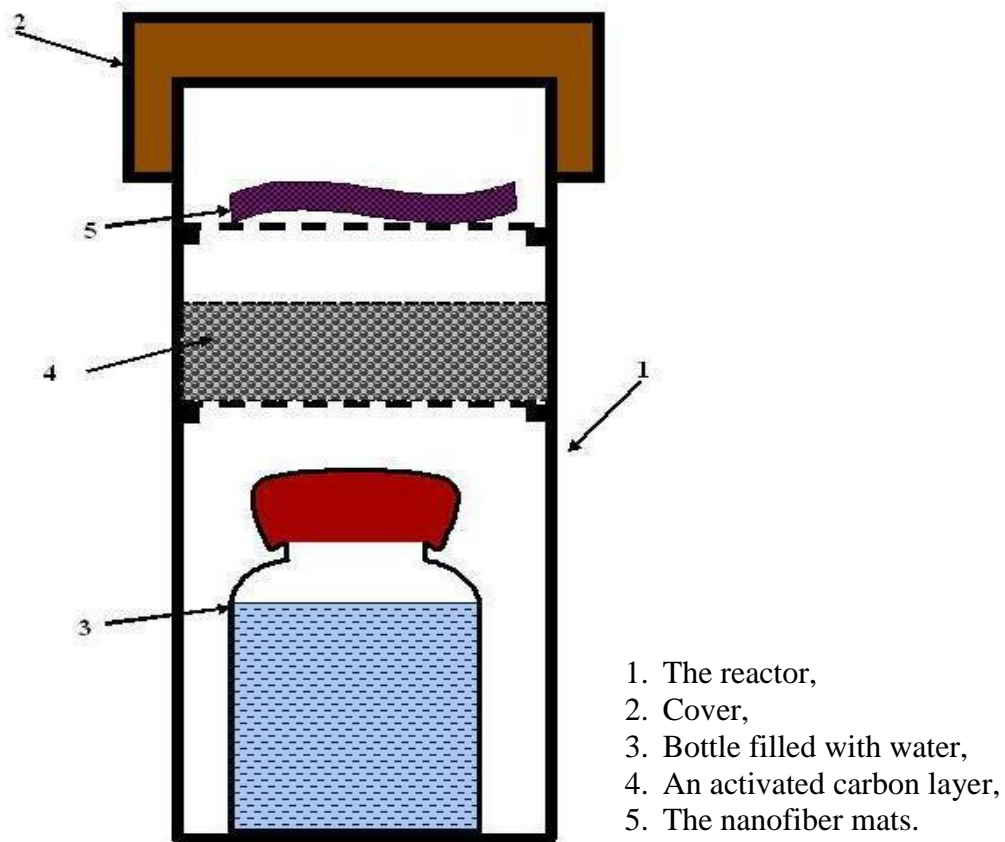


Figure 2: Schematic diagram for the especially designed reactor to perform a reaction between water vapor and hot carbon to produce water gas.

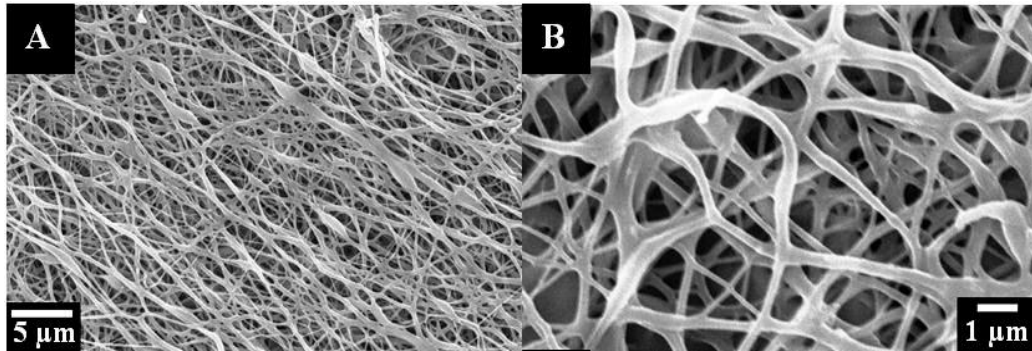


Figure 3: SEM images of silver nitrate/PVA dried nanofiber mats in two magnifications

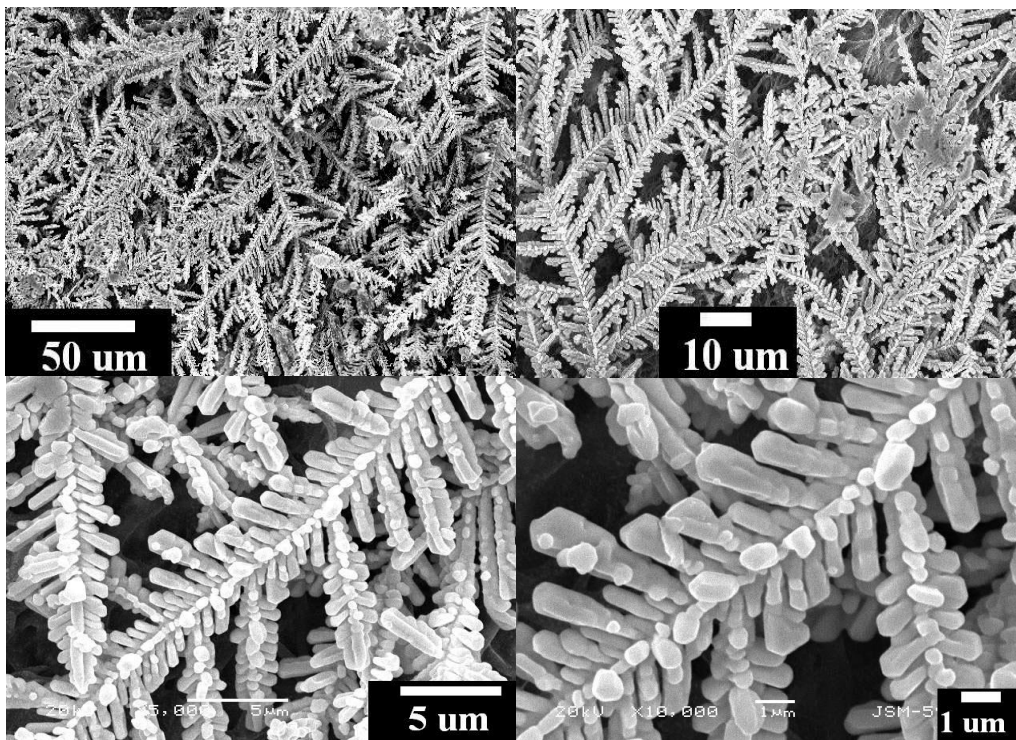


Figure 4: SEM images for the obtained nanoparticles after the proposed hydrothermal treatment methodology

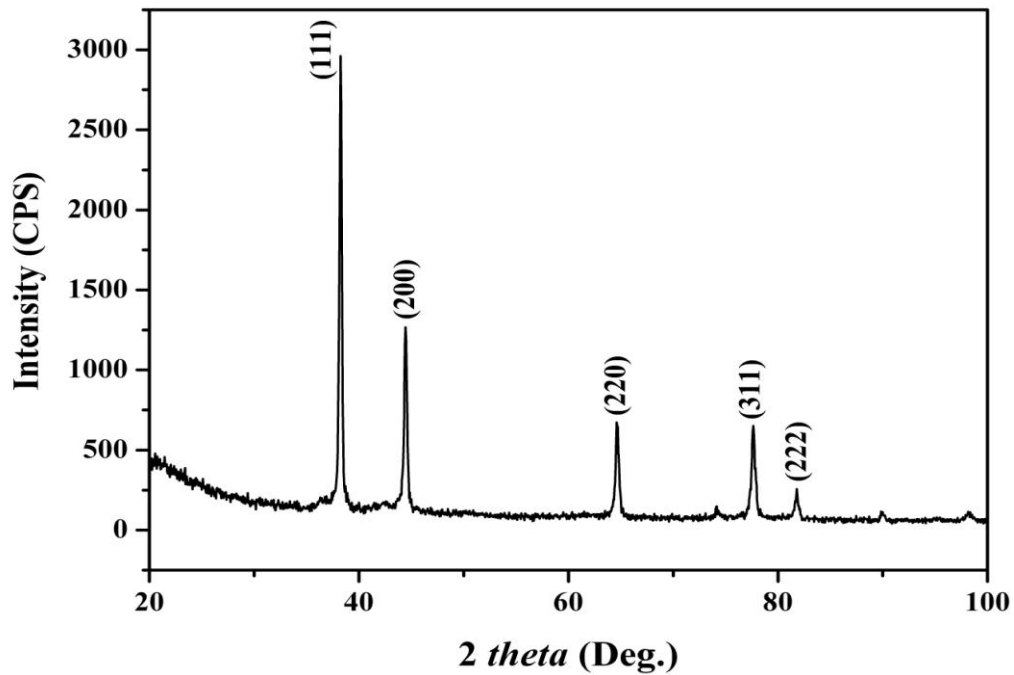


Figure 5: XRD data for the obtained nanofibers after calcination at 850 °C in Ar atmosphere, (111), (200), (220), (311) and (222) represent the main crystal planes in a pure silver crystals.

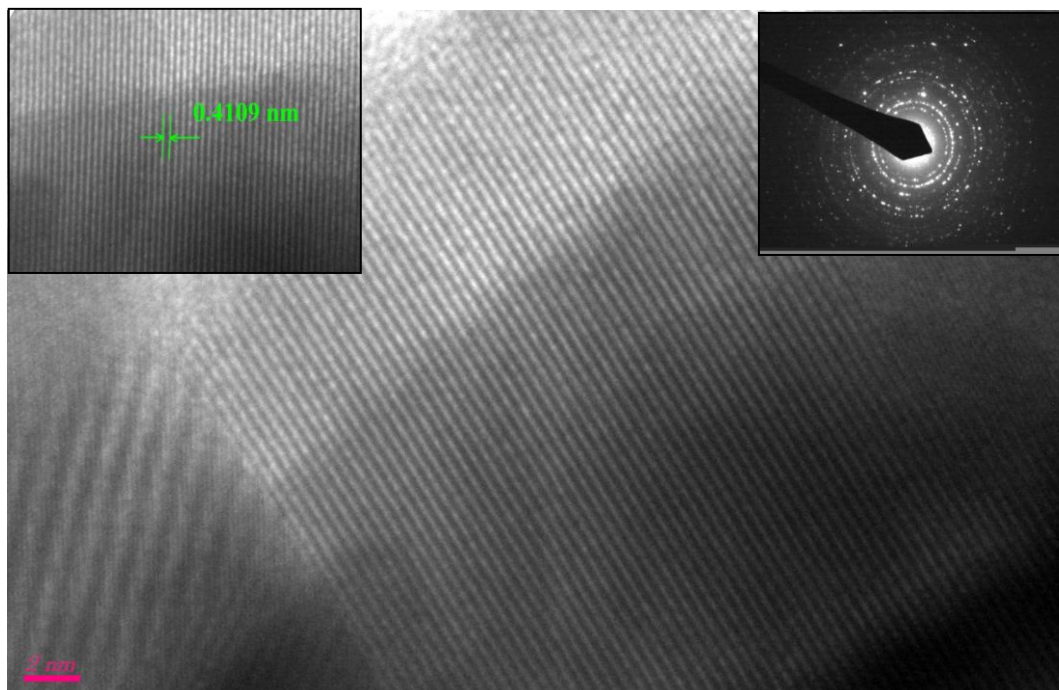


Figure 6: HR-TEM image for the obtained silver nanofibers, upper-left inset shows the FFT image and the upper-right one represents the selected area electron diffraction pattern.

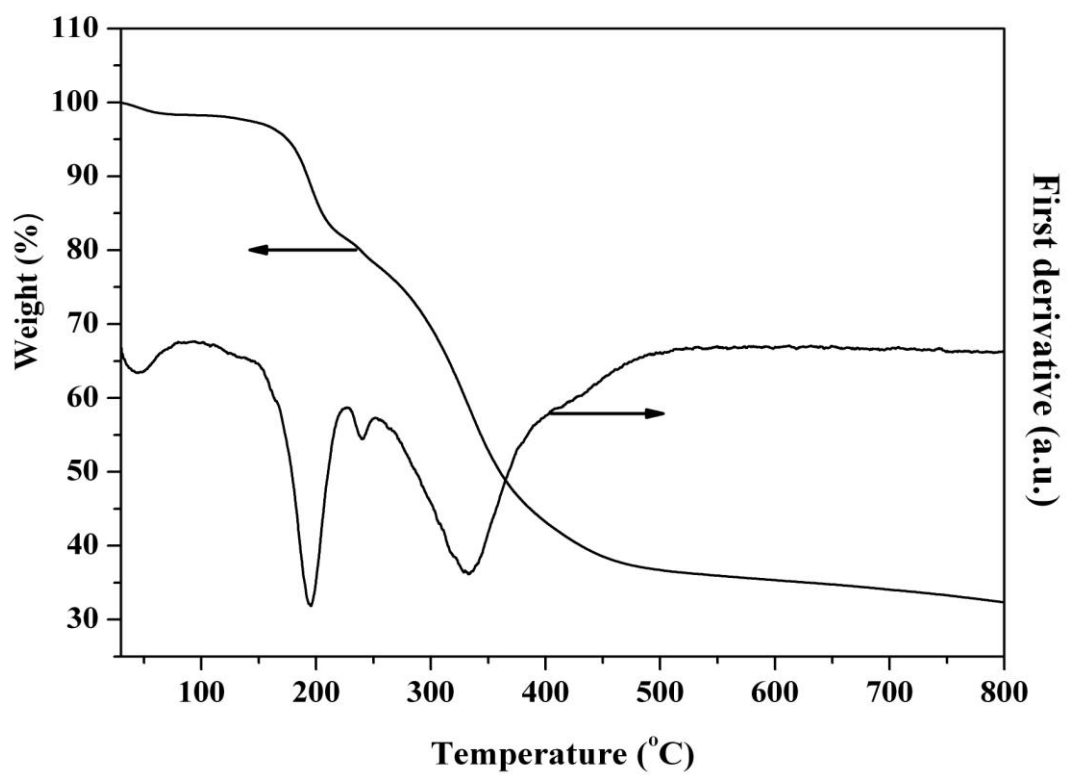


Figure 7: Thermal gravimetric analysis data and the corresponding first derivative of silver nitrate/PVA nanofiber mats.

**Military Technical College
Kobry El-Kobbah,
Cairo, Egypt**



**5th International Conference
on
Chemical & Environmental
Engineering
25 - 27 May, 2010.**